wjert, 2024, Vol. 10 Issue 8, 131-154 Original Article ISSN 2454-695X

World Journal of Engineering Research and Technology
WJERT
www.wjert.org
SJIF Impact Factor: 7.029

ENHANCED TORQUE RIPPLE MINIMIZATION IN SWITCHED RELUCTANCE GENERATORS USING ANT COLONY OPTIMIZATION

Zainab Musa Gwoma[1]*, S. Saidu Adamu[2], M. Buhari[3] and Abdulrahman Buji Babagana[4]

[1,2,3]Department of Electrical Engineering, Faculty of Engineering, Bayero University Kano, Kano State of Nigeria.

[4]Faculty of Engineering, University of Strathclyde, Glasgow, United Kingdom.

Article Received on 21/06/2024 **Article Revised on 11/07/2024** **Article Accepted on 31/07/2024**

***Corresponding Author**
Zainab Musa Gwoma
Department of Electrical Engineering, Faculty of Engineering, Bayero University Kano, Kano State of Nigeria.

ABSTRACT

Switched Reluctance Generators (SRGs) have gained significant attention in recent years due to their high reliability, low cost, and simple architecture. However, one of the major challenges associated with SRGs is the occurrence of torque ripple caused by its inherent non-linearity due to excessive magnetic saturation, as well as its doubly salient pole structure, which affects the generator's performance and efficiency. In this research work, we propose a PI- tuned Ant Colony Optimization (ACO) Technique to minimise the Torque Ripple on SRGs. The proposed Optimization framework will optimize the design parameters of the SRG, with emphasis on: Turn-On/Off angles and Reference current. MATLAB/Simulink Programming software was used to implement this technique on a typical 60kW, 4-phase, 8/6 Generator model with parameters as shown in table 1 of this paper. The Generator model was executed for about 6 possible arrangements of Reference Currents as well as firing angles at a speed of 5500 rpm, a 240 v excitation and at a current of 200 A. A comparison on the Performance of the SRG at these instances in the context of Generator flux, Generator Current, Torque Ripple as well as Generator speed were also presented and it reveals that the first set of optimal values corresponding to Figure (8) in the text, with I_{ref} = 145A, and firing angles, $\alpha = 61.37^{0}$ and $\beta = 87^{0}$ gives the best performance

with a convergence time of 0.09s and the average value of Torque during Convergence was 12.5227 Nm. It is expected that the results of this research work will provide valuable insights to researchers on the use of the Enhanced ACO for torque ripple minimization in SRGs.

KEYWORDS: Switched Reluctance Generators, Ant Colony Optimization, Torque Ripple Minimization, and Turn on and Turn off angle.

INTRODUCTION

Switched Reluctance Machines (SRMs) have been dominantly used in motoring mode. Many studies on reducing torque ripples in a motoring mode have been carried out extensively (Shin, Park, & Lee, 2015) (Husain & Ehsani, 1996). However, the resources on the minimization of torque ripples of the SRG for wind energy application are limited as most of the researches focuses on the operation of the machine as a motor. Their commercial application can be seen in vacuum cleaner, refrigerator, washing machine and electric vehicles (Pires, Pires, Cordeiro, & Foito, 2020) There is therefore a need for the torque ripple to be overcome to promote the application of the SRG in the generating mode of operation. (Gwoma, Popoola, Adamu, & Buhari, 2023).

Torque ripple is a fluctuation in the output torque of the generator, which occurs due to the non-linear magnetic characteristics of the SRG. Several methods have been proposed to minimize torque ripple in SRGs, including optimization techniques, such as genetic algorithms (GA), particle swarm optimization (PSO), and artificial neural networks (ANNs). However, these techniques have some limitations, such as high computational complexity and slow convergence rate (Pires et al., 2020) (Bao, Qi, & He, 2020) (Tariq, Muzzammel, Alqasmi, & Raza, 2020).

To mitigate torque ripple in switched reluctance generators effectively, advanced optimization techniques are essential. Ant Colony Optimization (ACO) is one such powerful metaheuristic algorithm inspired by the foraging behaviour of ants (Geng, Weng, & Liu, 2011) (Blum, 2005). ACO mimics the collective decision-making process of ants searching for the shortest path to a food source (Geng et al., 2011). In the context of SRG torque ripple minimization, ACO can be harnessed to intelligently explore the design space and find optimal configurations that lead to reduced torque ripple and improved generator performance.

This study focuses on employing ACO to optimize the design parameters and operating conditions of switched reluctance generators, with the ultimate goal of minimizing torque ripple. By leveraging the efficiency and effectiveness of ACO, this research aims to enhance the performance and applicability of switched reluctance generators in modern Energy Systems.

METHODOLOGY

This paper introduces a PI tuned Ant Colony Optimization Approach to Torque Ripple Minimization in SRGs in which the ACO is initialized by setting the upper and lower boundary values for the optimization. The ACO algorithm computes the first values for the reference current, turn ON angle, and turn OFF angle. A check for optimality of these values is performed. If optimality is not attained, the computed values are fed to a copy of the SRG design to update the values of the reference current, turn ON angle, and turn OFF angle in the generator. These values are used in the SRG to compute the corresponding torque of the generator and positions. These values are fed back to the ACO which is in turn utilised as update values in the iteration for optimizing the reference current, turn ON angle, and turn OFF angle. A check is performed again for the optimality of these values. If the optimality is not attained the process repeats itself. However, when optimality is attained, the optimal values are fed to the SRG design and the process exits. This is as shown in figure 1.

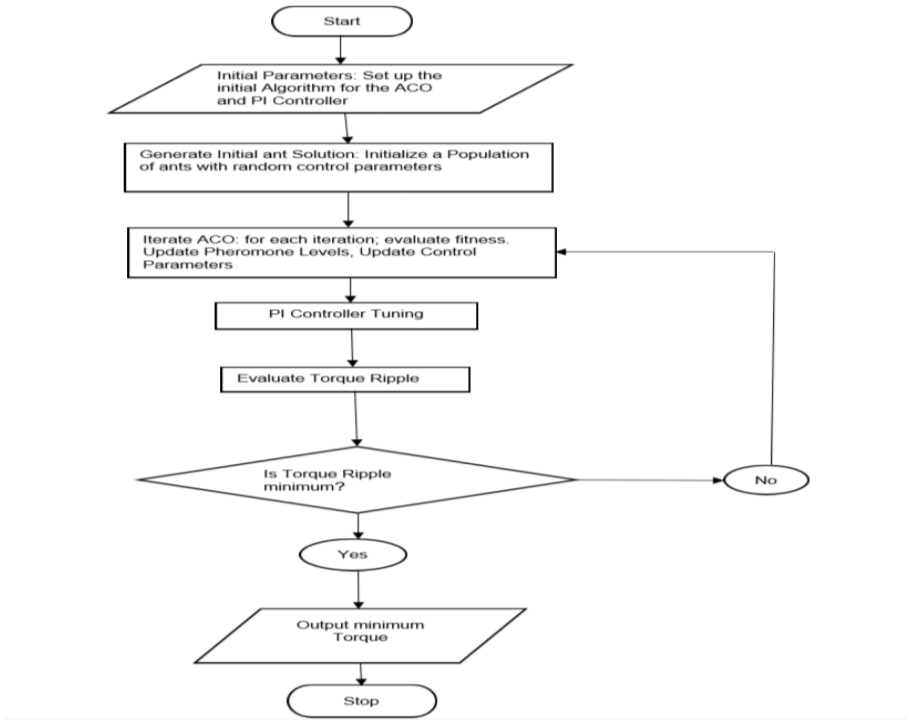

Figure 1: The flow chart algorithm implemented.

These steps are further explained explicitly in the pseudocode below:

1. Start

2. Initialize Parameters

- Set up the initial parameters for the ACO algorithm and the PI controller.

3. Generate Initial ant Solution

- Initialize a population of ants with random control parameters.

4. Iterate ACO

- For each iteration.

  - Evaluate Fitness
    - Simulate the switched Reluctance Generator with the current control parameters.
    - Calculate Torque ripple as the fitness metric.

  - Update pheromone levels
    - Update Pheromone levels based on ant Performance.

  - Update control Parameters:
    - Update ant solutions based on pheromone levels and local information.

5. PI Controller Tuning:

- Implement a PI Controller with the updated parameters from the ACO algorithm.
- Simulate the generators performance with the PI Controller.

6. Evaluate Torque Ripple

- Calculate Torque ripple using simulation results.

7. Convergence Check

- Check if convergence criteria are met, e.g. (Torque ripple is minimum, or maximum number of iterations are reached).
- If not converged, go back to step 4; else

8. End.

Switched Reluctance Generators

The SRG is referred to as a doubly salient pole due to the salient pole of its stator and rotor structure (Ganji, Heidarian, & Faiz, 2015) (Neto, Barros, De Paula, De Souza, & Filho, 2018) Salient pole refers to the structure of the element protruding from the yoke into the air gap. The rotor and the stator are made of steel laminations, and only the stator poles have windings concentrated around it. The rotor, on the other hand, is free from windings, magnets and brushes (Lobato, Cruz, Silva, & Pires, 2005) (Arifin, 2012) (Torrey, 2002).

SRGs have drawn great attention from industry and researchers due to its simple construction and lack of winding and permanent magnets on its rotor. The SRG has many advantages over other traditional dc or ac generators. This machine has simple and robust construction, high reliability and efficiency and low production cost (Susitra, Jebaseeli, & Paramasivam, 2010). Because the majority of the losses occur only in its stator, the SRG is relatively easy to cool down (Nassereddine, Rizk, & Nagrial, 2009). Hence, it can operate in high temperature and harsh environments. Furthermore, unlike conventional three phase generators such as the Induction Generator (IG) or a Permanent Magnet Synchronous Generator (PMSG), each phase of the SRG is controlled independently (Chwa & Lee, 2010). The magnetic independence among phases permits the machine to keep operating when phase-locking faults occur. This leads the SRG to have a better fault tolerance ability (Arifin, 2012) (Pierre, Gilles, Théophile, & Antoine, 2019) (Anekunu, 2015) SRG has been pointed out as a good alternative for wind energy conversion system (WECS) as it operates over a wide speed range at a high performance level (Omaç & Cevahir, 2021). The machine structure of a four-phase 8/6 poles SRG and the circuit diagram of the Power Converter, which facilitates the conversion of the unregulated output of the SRG, into a more suitable and regulated form for connection to electrical grid or some other purposes are as shown in figures 2 (a) and (b) respectively.

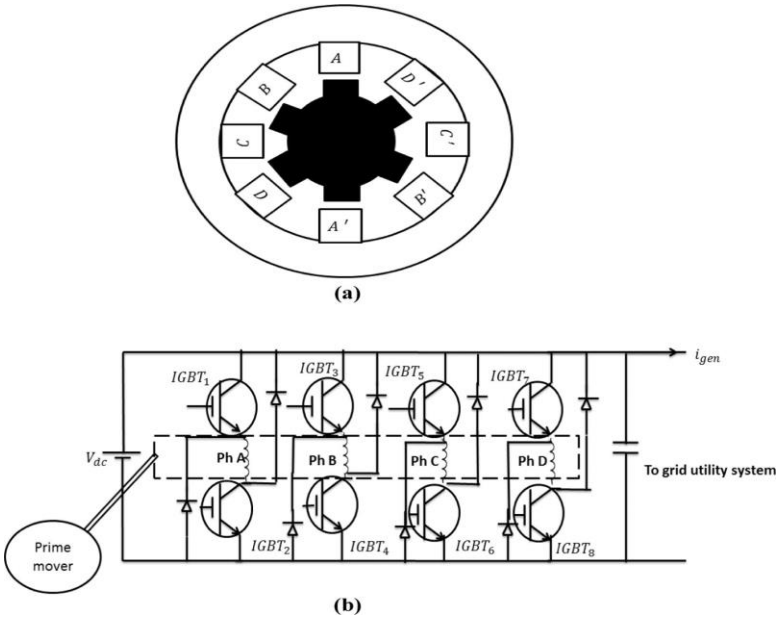

Fig. 2: A four-phase 8/6 poles SRG (a) Machine structure. (b) Power converter (Saad, El-Sattar, & Metally, 2018).

The phase inductance is maximum while the reluctance is minimum when the stator and rotor poles of SRG are in a completely aligned position. As the rotor pole leaves the aligned position, the stator windings current decreases and the inductance reaches its minimum value (Metally, Saad, & El-sattar, 2017) Torque generation in SRG depends on the magnetic field which tends to bring the poles to the minimum reluctance position. The SRG produces torque through excitation that is synchronized to rotor position (Metally et al., 2017) As the poles are separated, the reluctance begins to increase, creating a negative torque.

The torque generated by a phase under linear operating conditions in SRG is calculated as in equation (1).

$$T_e = \frac{1}{2} i^2 \frac{dL}{d\theta} \quad \text{..... (1)}$$

Where, T_e, i, L and h refers to the electromagnetic torque, phase current, phase inductance, and rotor position, respectively.

Since the SRG operates in the range where the inductance value decreases (dL/dh < 0), the resulting torque is negative. The total torque generated by the 3-phase generator used in this study is equal to the sum of the individual torques produced separately by the phases.

$$T_e = T_a(\theta, i_a) + T_b(\theta, i_b) + T_c(\theta, i_c) \quad \text{..... (2)}$$

The equation calculating the total torque can be shown as in (2). When the stator and rotor poles are moving away from each other due to energizing windings of the machine used as a generator, the torque of SRG is negative. In SRG, the winding of each phase must be energized sequentially. During the operation of the SRG, an electronic driver circuit is needed to enable current to flow through the phases sequentially according to the rotor position. Very different driver circuits for switched reluctance machines (SRM) control can be found in (Anekunu, 2015). In this study, the asymmetric bridge (AB) converter shown in Figure 1.(b) was used to drive the SRG. This driver circuit has two diodes and two switches per phase.

The equation showing a phase voltage of the SRM is given in (9).

$$V = R.i + \frac{d\Psi}{dt} \quad \text{(3)}$$

Where, V, i, R, L, h, and Ψ refer to the voltage applied to a phase winding, phase current, phase resistance, phase inductance, rotor position, and magnetic flux, respectively. In addition, it can be expressed as

$$\Psi = L(i,\theta).i \quad \text{(4)}$$

$$V = R.i + L\frac{di}{dt} + i\frac{d\theta}{dt}\frac{dL}{dt} \quad \text{(5)}$$

$$\omega = \frac{d\theta}{dt} \quad \text{(6)}$$

If the voltage equation of the SRM is rearranged using equation (4), (5) and (6), equations (7) and (8) are obtained.

$$V = R.i + L\frac{di}{dt} + i.\omega\frac{dL}{d\theta} \quad \text{(7)}$$

$$V = R.i + L\frac{di}{dt} + e \quad \text{(8)}$$

$$e = \omega.i.\frac{dL}{d\theta} \quad \text{(9)}$$

Where, e is the back electromotive force (emf) expressed as in (9) by using ω, the rotational speed (Zainab M. Gwoma, Musa Mustapha, Umar A. Benisheikh, Babangida Modu, 2017).

High Torque Ripple in SRGs

Despite all of these advantages stated earlier, it has not been widely employed in the industry owing to its high torque ripple which causes acoustic noise and oscillations (Frikha et al.,

2023) One of the two major causes of high torque ripple is the SRG's very high nonlinear characteristics due to its excessive magnetic saturation (Ro, Lee, Lee, Jeong, & Lee, 2015). This non linearity causes torque ripple when each phase is controlled with a constant square current waveform. The other major cause of the torque ripple is due to the doubly salient pole structure of the SRG as it has its stator and rotor poles protruding into the air gap (Ganji et al., 2015). The high torque ripples are caused during phase commutation period when the torque production is being transferred from the outgoing phase to the incoming phase (Palanimuthu et al., 2022). The general control model for SRG is as shown in figure (3).

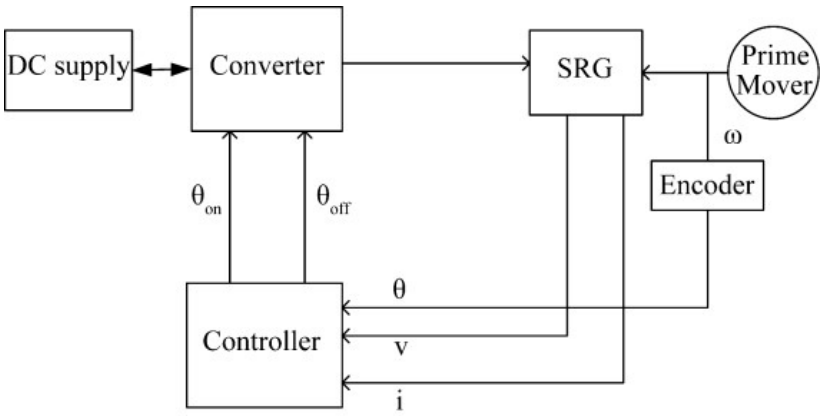

Figure 3: Basic control model for SRG (Gwoma et al., 2023).

SRG produces negative torque when the phase is excited as the rotor pole moves through the aligned position. At this moment, energy is extracted from the prime mover.

Torque ripple is affected by the current conduction interval and by the relative position between phases. The torque ripple (T_{ripple}) can cause damage to the SRG structure, besides the machine's life reduction, and it is defined as

$$T_{ripple} = \frac{T_{max} - T_{min}}{T_{avg}} \quad \ldots\ldots\ldots\ldots\ldots\ldots\ldots\ldots\ldots\ldots\ldots\ldots\ldots\ldots\ldots\ldots (10)$$

Where T_{max} and T_{min} are the maximum and minimum torque, respectively and T_{avg} is the average torque. (Neto et al., 2018).

To improve the performance of the SRG, both the efficiency and the torque ripple must be optimized. These parameters are strictly related to the SRG firing angles and the DC link voltage, besides the rotor speed. Moreover, these parameters must be properly chosen (Xu, Shang, Chen, Zhu, & Han, 2019).

Swing Equation

Swing equations are a set of differential equations used to model the dynamic behaviour of synchronous generators in power systems (Padiyar, 2008). The term swing refers to the angular displacement of the generator rotor from its synchronous position. Swing equations help to analyse the transient stability of power systems following disturbances such as sudden load changes, faults, or other disruptions. Transient stability refers to the ability of the power system to return to a stable operating condition after being subjected to a disturbance (Prabha Kundur, 1994). The swing equations are derived from the mechanical and electrical dynamics of the synchronous generator. They are typically represented in terms of differential equations that describe the dynamics of the generator's rotor angle and speed. The basic form of swing equation is as expressed in equation (11).

$$M\frac{d^2\delta}{dt^2} = P_m - P_e \ldots\ldots\ldots\ldots\ldots\ldots\ldots\ldots\ldots\ldots\ldots\ldots (11)$$

Where: **M** is the inertia constant of the Generator, $\boldsymbol{\delta}$ is the rotor angle (angle difference between the rotor and the synchronous position), **t** is time, $\boldsymbol{P_m}$ is the mechanical power input to the generator, $\boldsymbol{P_e}$ is the electrical power output of the generator, which depends on the generator's internal voltage and the power delivered to the connected grid.

When there is an unbalance between the torques acting on the rotor of the generator, the net torque causing acceleration or deceleration is expressed as

$$T_a = T_m - T_e \ldots\ldots\ldots\ldots\ldots\ldots\ldots\ldots\ldots\ldots\ldots\ldots\ldots (12)$$

Where: T_a= accelerating torque in N.M,

T_m= Mechanical Torque in N.m

T_e = Electromagnetic Torque in N.m

$$\frac{d\Delta\bar{\omega}r}{dt} = \frac{1}{2H}(\bar{T}m - \bar{T}e - K_D\Delta\bar{\omega}r) \ldots\ldots\ldots\ldots\ldots\ldots (13)$$

$$\frac{d\delta}{dt} = \omega_0\Delta\bar{\omega}r \ldots\ldots\ldots\ldots\ldots\ldots\ldots\ldots\ldots\ldots\ldots\ldots\ldots\ldots (14)$$

From equation (12), T_m *and* T_e are positive for a generator and negative for a motor. Since the combined inertia of the generator and the prime mover is accelerated by the unbalance in the applied torques, the equation of motion is hence as expressed in equation (13) and (14), in pu. (Prabha Kundur, 1994).

State of the Art in SRG Designs

Different researches have been carried out on torque ripple minimization of the SRM in the motoring and generating mode of operation using conventional and heuristic optimization techniques. An extensive review of Torque Ripple Minimization Strategies on Switched Reluctance Machines was carried out by (Prabha Kundur, 1994) discussing the different strategies with their pros and cons. Author (Zhang, Yang, Ma, Lin, & Yang, 2019) proposed the use of linear TSF, where the torque references of commutating phases are assumed to vary linearly. A control algorithm was also presented to calculate the angles and current references offline for a given torque reference. The use of sinusoidal TSF is proposed in (Husain, 2002) to address the issue of torque ripple, especially at low speeds. This helped simplify and reduce the computational burden, however, the main drawback in this method is the use of a linear motor model for generating current profiles. (Husain & Ehsani, 1996) Proposes a TRM by use of PWM phase control optimal profiling. A control algorithm was presented to calculate the angle and current reference for a given torque reference. (D S Reay, Green, & Williams, 1993) Proposes a Neural Network TRM by generating current profiles for a particular reference through online learning. This avoided calculation and storage of current profiles. (Donald S Reay, Mirkazemi-moud, Green, & Williams, 1995) Proposes the use of fuzzy adaptive system for current profile online learning of TRM. The adaptive system develops and tunes the fuzzy rules and adjustment of weights at the output of the fuzzy system was done the least mean square (LMS) algorithm. (Sahoo, Dasgupta, Panda, & Xu, 2012) Proposes TRM by use of TSF and PWM based robust DTC. In [18], a robust TRM method is proposed based on a self-tuning neuro fuzzy logic compensator. The dc component of the torque was removed such that only the ripple remains. Ref. (Shahbazi, 2021) proposes an enhanced DITC TRM by adding a PI controller before instantaneous torque control and simulated using MATLAB/Simulink. In (Mousavi-Aghdam, Feyzi, & Ebrahimi, 2012), an adaptive neuro-fuzzy inference system (ANFIS) approach was employed and the dynamic behaviour of the motor improved, with no overshoot and a good rejection of impact load disturbance, thus leading to a better performance and higher robustness. Ref (Bolognani & Zigliotto, 1996) uses speed error as input and the reference current as output, which was modulated by subtracting the output of the fuzzy system from the sum of four phase currents computed at the previous sampling period. The modulated current was then fed into the phase windings of the motor through a converter, thus maintaining the speed constant and reducing the torque ripples.

Satisfactory control performance is difficult to achieve using traditional controllers such as the proportional, integral and/or derivative (PI, PD, and PID) controllers as they can only be tuned to obtain desired performance under a specific set of operating conditions. However, its performance deteriorates significantly as the operating conditions vary with increasing nonlinearity of the SRG. Hence, artificial intelligence control techniques such as Fuzzy Logic(FL) (Arifin, 2012) (Tavakkoli & Moallem, 2012) Artificial Neural Network (ANN) (Tavakkoli & Moallem, 2012) (Hasanien & Muyeen, 2012) Bacteria Foraging Optimization (BFO) (Hajiabadi, Farshad, & Shamsinejad, 2021), Genetic Algorithm (GA) (Lai, Feng, Iyer, Mukherjee, & Kar, 2017) are employed for torque ripple minimization which allows for better performance. (Geng et al., 2011) Suggested ACO for solving the traveling salesman problem. For global optimization of multimodal continuous objective functions of the SRG, it is difficult to use deterministic methods to obtain global solutions. Hence, increasing efforts are devoted to the development of heuristic and meta-heuristic algorithms. The most notable progress in this respect is the development of evolutionary methods. Recently, a new entrance to the family of evolutionary algorithms, the ant colony optimization (ACO) method (Blum, 2005) (Gwoma et al., 2023) (Geng et al., 2011).

Seen from the artificial intelligence (AI) perspective, ACO algorithms are one of the most successful strands of swarm intelligence. The goal of swarm intelligence is the design of intelligent multi-agent systems by taking inspiration from the collective behaviour of social insects such as ants, termites, bees, wasps, and other animal societies such as flocks of birds or fish schools (Blum, 2005). Examples of swarm intelligent algorithms other than ACO are those for clustering and data mining inspired by ants' cemetery building behaviour, those for dynamic task allocation inspired by the behaviour of wasp colonies, and particle swarm optimization (Choi & Koh, 2006).

Ant Colony Optimization (ACO) belongs to the class of biologically inspired algorithms and represents a commonly deployed cooperative, multi-agent, Meta-heuristics to tackle combinatorial optimization problems. ACO models the communication behaviour observed in ant colonies and is inspired by the capability of real ants to find the shortest path between their nest and a food source in a relatively short time (Geng et al., 2011) This is achieved by means of indirect communication among ants that is triggered by a chemical indicator referred to as pheromone that positively influences the random path selection.

Premature convergence and poor exploitation are the main obstacles for the heuristic algorithms. ACO technique is effective and efficient in dealing with premature convergence or poor exploitation, and it has an advantage of not translating the real data into code, as compared with genetic algorithms (Husain, 2002) Hence, suitable for use on Switched Reluctance Machines (SRMs) for Torque Ripple Minimization (TRM).

The ACO is designed to emulate the PI controller for closed loop operation under different wind speed condition. Parameter tuning using ACO can be computationally intensive, but can help to discover optimal or improved control parameter values that might be difficult to find manually or through other optimization methods.

In search for a more complete partial solution $S_{k,n}$, ants progress to the next node by determining a set of feasible expansions $\Omega_{k,n}-1$ from $S_{k,n}-1$. An ant choses an expansion $j \epsilon \Omega_{k,n} - 1$ according to a probabilistic function p that represents a biased probability distribution of the relative attractiveness of the expansion and the relative trail pheromone level (Geng et al., 2011). The attractiveness is represented by a heuristic function η that serves as a problem specific indicator for the added value of having j in $S_{k,n}$. The trail pheromone level τ describes how proficient j has been in the past for finding an optimal solution. These terms are as expressed in equation (20).

$$P_k(i,j) = \begin{cases} \dfrac{[\eta(i,j)]^{\alpha}[\tau(i,j)]^{\beta}}{\sum g \in \Omega_{k,n-1}[\eta(i,g)]^{\alpha}[\tau(i,g)]^{\beta}} & , \quad j \in \Omega_{k,n-1} \\ 0 & , \quad else \end{cases} \tag{20}$$

The probability p_k (i,j) for an ant k to choose an expansion j from the feasible expansion set $\Omega_{k,n}-1$ from a node i is hence calculated using equation (20); Where the parameters α and β define the relative importance of the heuristic information compared to the pheromone concentration (Ditze, 2007) (Blum, 2005).

Unlike most previous studies in which the effect of only one of those angles are considered, this paper also examines the simultaneous performance of both the Turn-on and Turn-off angles which brings about a better evaluation of the SRG.

For each combination of speed and torque, the enhanced ACO simulates the Model, gets outputs and determines the value of the objective function subject to constraints. The ACO

continuously changes the firing angles (θ_{on} θ_{off}) until the optimum firing angle that gives best performance or reaches maximum iteration is attained.

The average torque (T_{ave}), torque ripple (T_{ripple}), and the efficiency (η) of the SRG are mixed in a multi- objective function (F) as presented in equations (21) – (27).

$$T_{ave} \frac{1}{\tau}\int_0^{\tau} T_e(t)\,dt \quad (21)$$

$$T_{ripple} = T_{max} - T_{min} \quad (22)$$

$$T_Q = T_{ave} - w_r(T_{max} - T_{min}) \quad (23)$$

$$\eta = \frac{\omega T_{ave}}{V_{dc} I_{ave}} \quad (24)$$

$$F = w_q \frac{T_Q}{T_{Qbase}} + w_e \frac{\eta}{\eta_{base}} \quad (25)$$

Also, $\theta_{cnd} = \theta_{off} - \theta_{on} \geq 30^0$ (26)

$$0 < I_{ref} \leq I_{ref}^{max} \quad (27)$$

Where: T_{max} and T_{min} are the highest and lowest values of the torque waveform (T_e) over one electric cycle (τ), T_Q is the Torque quality factor, ω is the Generator speed in rad/sec, V_{dc} is the voltage applied to the ABC, I_{ave} is the average value of the supply current, T_{Qbase} and η_{base} are base values of the torque quality and efficiency respectively. w_r, w_q and w_e are weighing factors. Considering equation (43), since more emphasis is on the torque quality, the value of w_q is higher than w_e. Also, from equation (44), a conduction angle of 30^0 was selected for the 4 phase, 8/6 SRG. For optimum performance, I_{ref} must be as expressed in equation (27).

SIMULATION RESULTS AND DISCUSSION

For this paper, a four Phase 8/6 SR Generator with parameters as shown in table 1 was adopted (Hajiabadi et al., 2021), and the ACO Parameters are as shown in table 2. The simulation and optimization Procedure for the PI tuned SRG Control system is as schematically illustrated in figure 4.

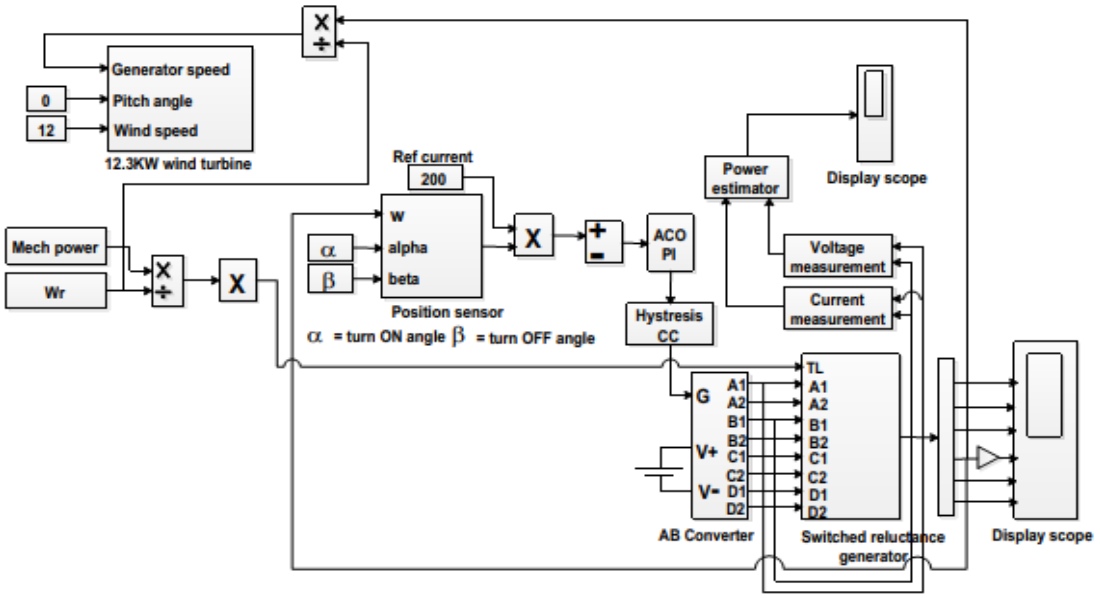

Figure 4: MATLAB -Simulink implementation of the Program.

The Generator model was executed for all possible arrangement of the firing angles at a speed of 5500 rpm, a 240 v excitation at a current of 200 A. It was evident that there is a pair of firing angles at which the Torque Ripples tends to be at its minimum. These are as shown in figure 5.

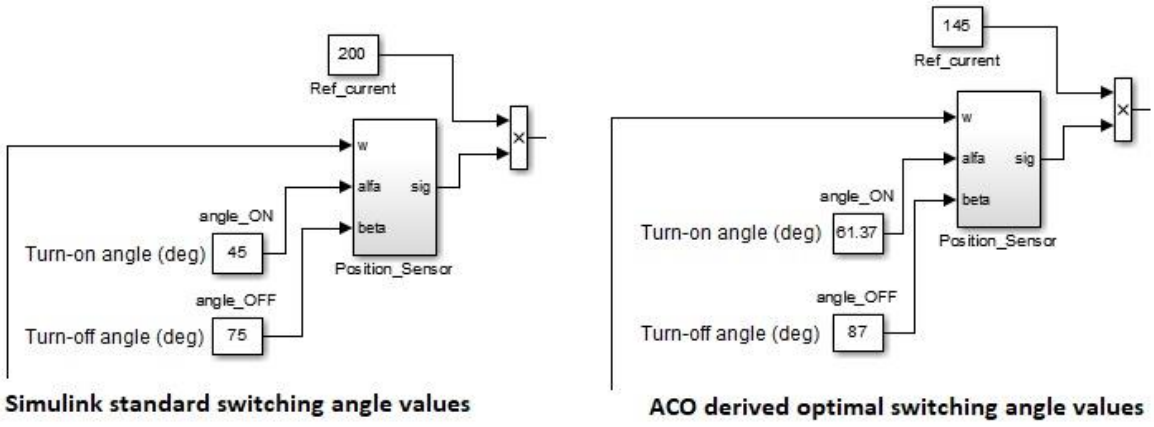

Figure 5: SIMULINK of PI-ACO Derived optimal Switching angles.

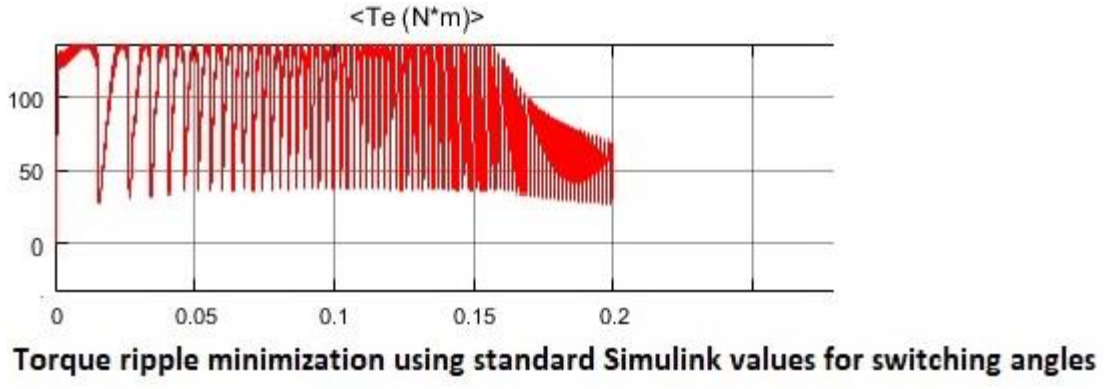

Figure 6: Waveforms obtained using Simulink derived values for switching angles.

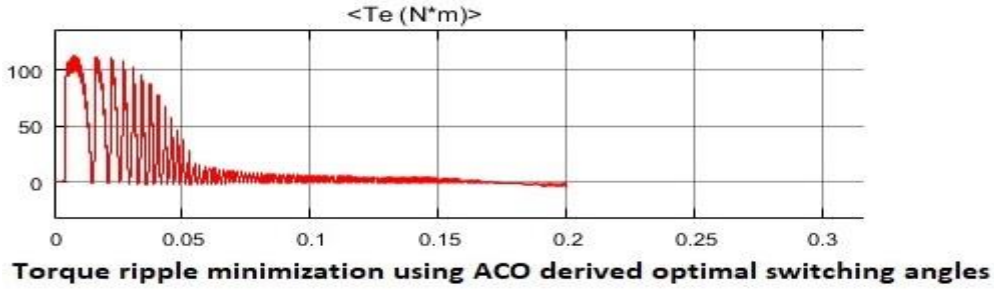

Figure 7: TRM technique using ACO derived Optimal Switching angles.

It can be seen from the waveforms of figure 6 and that of figure 7, how the torque ripples were drastically minimised using ACO with a better convergence rate as compared to the most recently published method.[81]

Performance of the SRG in the context of Generator flux, Generator Current, Torque ripple as well as speed were obtained at different stages of I_{ref} and firing angles during the simulation and are as shown in the following figures 8-13.

Figure 8 shows the performance of the SRG with I_{ref} = 145 A, $\alpha = 61.37^{0}$, $\beta = 87^{0}$. The torque ripple shown in Figure 8(c) is the focus of this analysis. It can be observed that the minimization of the torque ripple started from 0.03s. Convergence occurred at 0.09s. The average value for the torque at convergence is 12.5227 Nm.

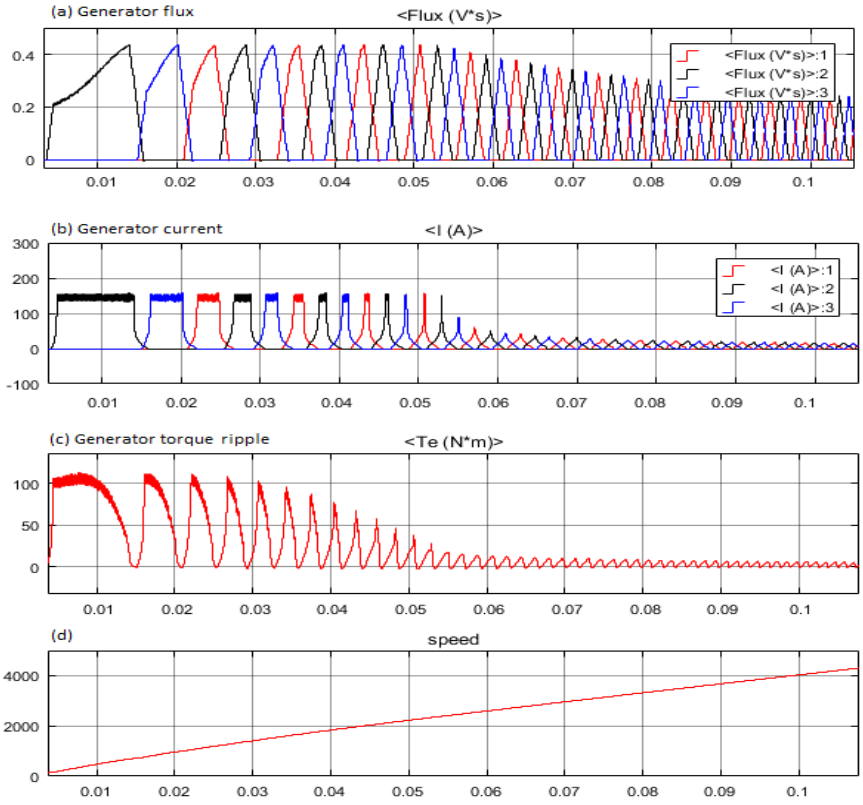

Figure 8: SRG performance for optimal values: I_{ref} = 145 A, α = 61.37 ^{0}, β = 87 ^{0}.

For SRG optimal performance for optimal values of I_{ref} = 43 A, α = 67.26 ^{0}, β = 120 ^{0}, minimization of the torque ripple started from 0.02s. The convergence occurred in the interval 0.07s to 0.1s with an average value of 1.7364 Nm during the interval; this is as shown in Figure 9.

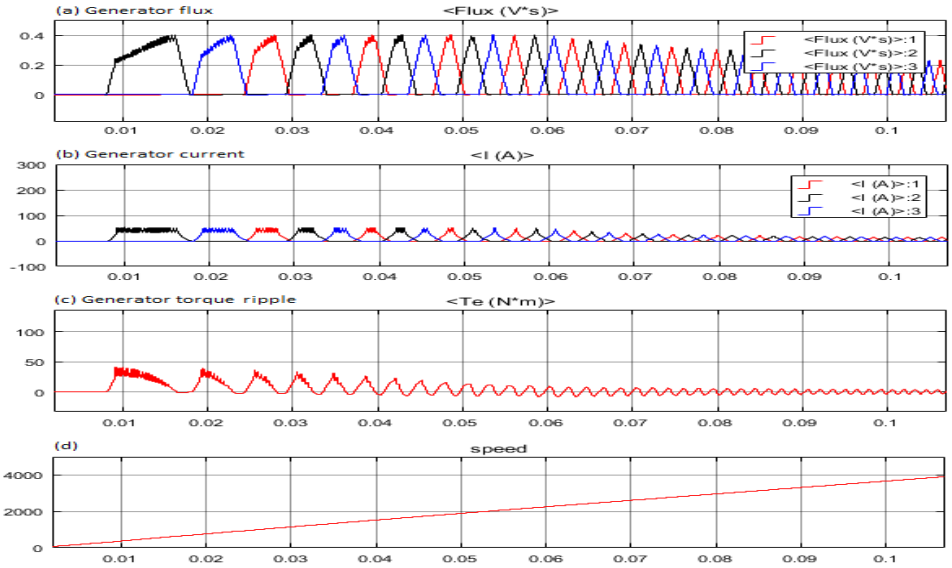

Figure 9: SRG performance for optimal values: I_{ref} = 43 A, α = 67.26 ^{0}, β = 120 ^{0}.

In Figure 10, the SRG optimal performance values are I_{ref} = 237 A, α = 48.45 ^{0}, β = 61 ^{0}, minimization of the torque ripple started from 0.05s the convergence occurred in the interval 0.16s to 0.22s with an average value of 35.2238 Nm during the interval.

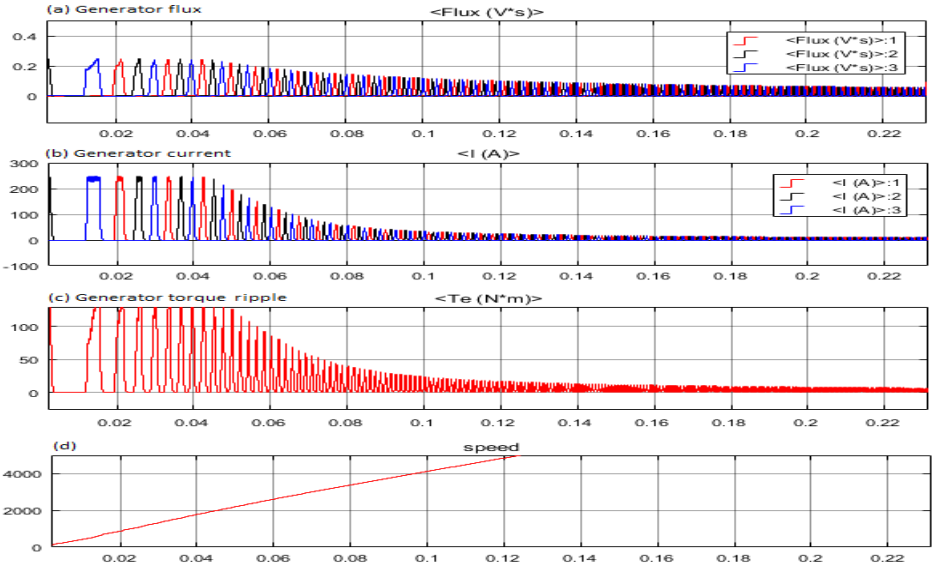

Figure 10: SRG performance for optimal values: I_{ref} = 237 A, α = 48.45 ^{0}, β = 61 ^{0}.

In Figure 11, it can be observed that minimization of the torque ripple started from 0.02s, convergence occurred between 0.06s and 0.1s with an average value of 15.8696 Nm. The performance of the SRG for the indicated optimal values shows that even though convergence was achieved, there was approximate no torque. This is a sub-optimal performance when the overriding objective is considered.

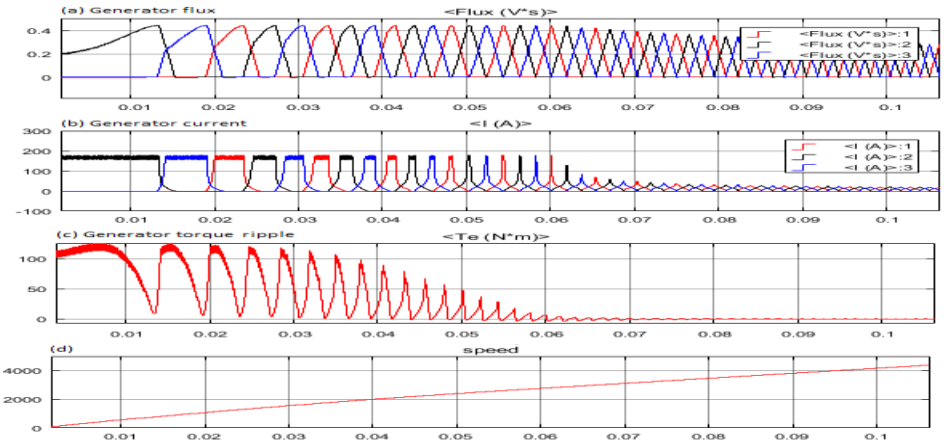

Figure 11: SRG performance for optimal values: I_{ref} = 167 A, α = 58.9 ^{0}, β = 120.75^0.

A similar convergence to Figure 11 can be observed in Figure 12. However, the torque showed higher magnitude in Figure 11 before the convergence which stabilized at 0.06s with an average value of 14.1306 Nm.

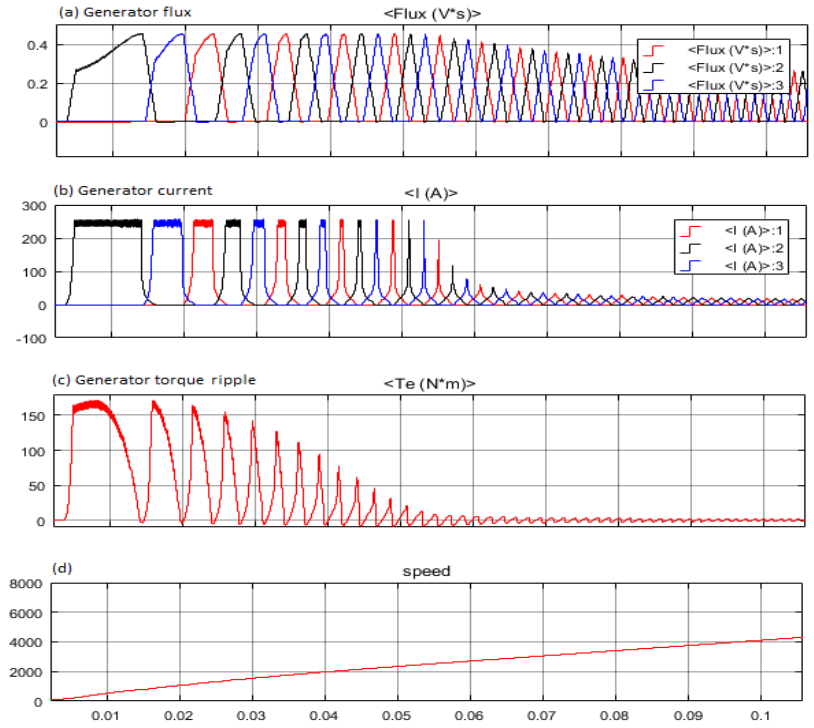

Figure 12: SRG performance for optimal values: I_{ref} = 245 A, α = 61.56 ^{0}, β = 99.75 ^{0}.

In Figure 13, minimization of the torque ripple started from 0.06s whereas convergence occurred between 0.2s and 0.22s, with an average value of 56.0988 Nm. Thus, the optimal values indicated in Figure 13 yields the highest torque value for the different set of optimal values obtained.

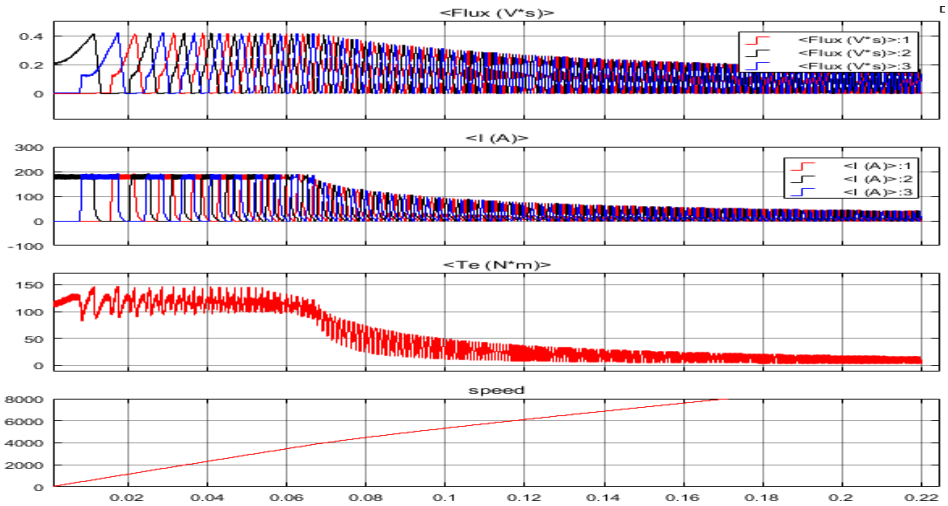

Figure 13: SRG performance for optimal values: I_{ref} = 179A, α = 40.28 ^{0}, β = 82 ^{0}.

Figure (14) shows a comparison of the set of six different optimal parameters obtained from the SRG simulation corresponding to Figures 8-13. It can be observed that for each data set, the turn OFF angle (β) is higher than the turn ON angle (α). For the SRG to operate with any of these values, higher latency will occur during the (β) operation by the SRG. A comparison of Figure 14(a) and 14(b) reveals that the first set of optimal values corresponding to Figure (8) gives the best performance from the perspective of convergence time and torque; the second set of optimal values, corresponding to figure (9) will be preferred from the perspective of I_{ref}, (α), and (β).

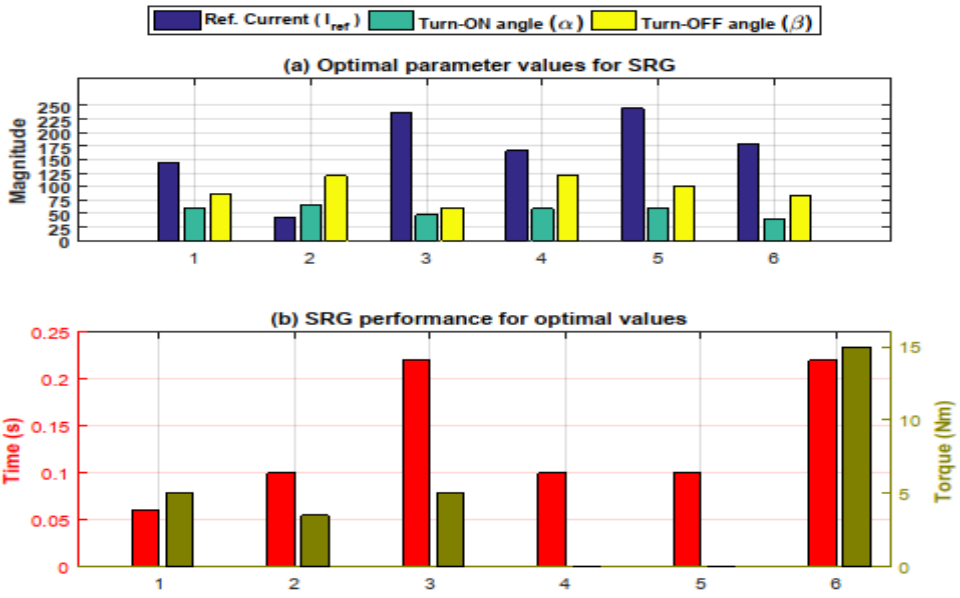

Figure 14: Optimal operating parameters of SRG.

Table 1: Four Phase 8/6 SRG Parameters.

S. No.	Parameter	Value
1	Nominal Power	60 Kw
2	Nominal Speed	5500 rpm
3	Max. Coil Current	450 A
4	Reference Current	200 A
5	Stator Coil Resistance	0.05 Ω
6	Coefficient of Inertia	0.05 kg.m^3
7	Coefficient of Friction	0.02 N.m.s

The Generator Specifications for the four Phase 8/6 Switched Reluctance Generator adopted.

Table 2: ACO Parameters.

S. No.	Parameter	Value
1	Number of ants (k):	30
2	Number of Particles /stage (i^{max}):	13
3	Number of Stages (i^{stage}):	4
4	Allowed Iteration per stage:	25
5	Pheromone scaling factor (ζ):	1.5
6	Pheromone Evaporation Rate (ρ):	0.2

The Ant Colony Optimization Parameters used.

CONCLUSION

A Torque ripple minimisation technique for a Switched Reluctance Generator using PI-Tuned, Ant Colony Optimization was presented in this paper. The results shown in this work indicates that PI-Tuned ACO technique applied to the switching angles of an SRG can reduce the Generator's torque ripples to the barest minimum. Ultimately, unlike similar works that have considered the performance of only one switching angle (either Turn on or turn off) such as in (Arifin, 2012) and (Xue, Cheng, & Ho, 2009); this paper considered the performance of both firing angles (both Turn-On and Turn-Off) simultaneously for a better performance and investigation. MATLAB/Simulink was used to implement this technique on a typical 60kW, 4-phase, 8/6 Generator with parameters as shown in table 1. The Generator model was executed for all possible arrangement of the firing angles at a speed of 5500 rpm, a 240 v excitation at a current of 200 A and the results confirmed validation of the method.

REFERENCES

1. Anekunu, A. Y. *Control of Switched Reluctance Generator for Wind Energy Applications*, 2015; *3*(9): 290–295.
2. Arifin, A. State of the Art of Switched Reluctance Generator. *Energy and Power Engineering*, 2012; *04:* 447–458. https://doi.org/10.4236/epe.2012.46059
3. Bao, G. Q., Qi, W., & He, T. Direct torque control of PMSM with modified finite set model predictive control. *Energies*, 2020; *13*(1). https://doi.org/10.3390/en13010234
4. Blum, C. Ant colony optimization: Introduction and recent trends. *Physics of Life Reviews*, 2005; *2*(4): 353–373. https://doi.org/https://doi.org/10.1016/j.plrev.2005.10.001
5. Bolognani, S., & Zigliotto, M. Fuzzy logic control of a switched reluctance motor drive. *IEEE Transactions on Industry Applications*, 1996; *32*(5): 1063–1068. https://doi.org/10.1109/28.536867
6. Choi, Y. K., & Koh, C. S. Pole Shape Optimization of Switched Reluctance Motor for

Reduction of Torque Ripple. *2006 12th Biennial IEEE Conference on Electromagnetic Field Computation*, 2006; 335. https://doi.org/10.1109/CEFC-06.2006.1633125

7. Chwa, D., & Lee, K.-B. Variable Structure Control of the Active and Reactive Powers for a DFIG in Wind Turbines. *IEEE Transactions on Industry Applications*, 2010; *46*(6): 2545–2555. https://doi.org/10.1109/TIA.2010.2073674
8. Ditze, M. Evaluation of an Ant Colony Optimization Based Schedulerfor the Transmission of Multimedia Traffic in the 802.11e Edca. *Proceedings of the 3rd ACM Workshop on Wireless Multimedia Networking and Performance Modeling*, 2007; 9–15. https://doi.org/10.1145/1298216.1298220
9. Frikha, M. A., Croonen, J., Deepak, K., Benômar, Y., El Baghdadi, M., & Hegazy, O. Multiphase Motors and Drive Systems for Electric Vehicle Powertrains: State of the Art Analysis and Future Trends. *Energies*, 2023; *16*(2). https://doi.org/10.3390/en16020768
10. Ganji, B., Heidarian, M., & Faiz, J. Modeling and analysis of switched reluctance generator using finite element method. *Ain Shams Engineering Journal*, 2015; *6*(1): 85–93. https://doi.org/10.1016/j.asej.2014.08.007
11. Geng, J., Weng, L., & Liu, S. An improved ant colony optimization algorithm for nonlinear resource-leveling problems. *Computers and Mathematics with Applications*, 2011; *61*(8): 2300–2305. https://doi.org/10.1016/j.camwa.2010.09.058
12. Gwoma, Z. M., Popoola, K. A., Adamu, S. S., & Buhari, M. A Review of Torque Ripple Minimization Strategies in Switched Reluctance Machines. *International Journal of Science and Engineering Invention (IJSEI)*, 2023; *09*(02): 8–17.
13. Hajiabadi, H., Farshad, M., & Shamsinejad, M. Multi-objective optimization and online control of switched reluctance generator for wind power application. *International Journal of Industrial Electronics Control and Optimization*, 2021; *4*(1): 33–45. Retrieved from https://ieco.usb.ac.ir/article_5425.html%0Ahttps://ieco.usb.ac.ir/article_5425_32f1e5399e74869363ac5e0c0cb427e8.pdf
14. Hasanien, H. M., & Muyeen, S. M. Speed control of grid-connected switched reluctance generator driven by variable speed wind turbine using adaptive neural network controller. *Electric Power Systems Research*, 2012; *84*(1): 206–213. https://doi.org/https://doi.org/10.1016/j.epsr.2011.11.019
15. Husain, I. Minimization of torque ripple in SRM drives. *IEEE Transactions on Industrial Electronics*, 2002; *49*(1): 28–39. https://doi.org/10.1109/41.982245
16. Husain, I., & Ehsani, M. Torque ripple minimization in switched reluctance motor drives

by PWM current control. *IEEE Transactions on Power Electronics*, 1996; *11*(1): 83–88. https://doi.org/10.1109/63.484420

17. Lai, C., Feng, G., Iyer, K. L. V., Mukherjee, K., & Kar, N. C. Genetic Algorithm-Based Current Optimization for Torque Ripple Reduction of Interior PMSMs. *IEEE Transactions on Industry Applications*, 2017; *53*(5): 4493–4503. https://doi.org/10.1109/TIA.2017.2704063
18. Lobato, P., Cruz, a., Silva, J., & Pires, A. The Switched Reluctance Generator for Wind Power Conversion. *9th Spanish Portuguese Congress on Electrical Engineering*, 2005; 1.
19. Metally, M. E., Saad, N. H., & El-sattar, A. A. *Sensorless Control of Switched Reluctance Generator with Maximum Power Extraction Wind Driven Based on MO-PSO*, 2017; *1*(10): 13–24.
20. Mousavi-Aghdam, S. R., Feyzi, M. R., & Ebrahimi, Y. A New Switched Reluctance Motor Design to Reduce Torque Ripple using Finite Element Fuzzy Optimization. *Iranian Journal of Electrical and Electronic Engineering*, 2012; *8*(1): 91–96. Retrieved from http://ijeee.iust.ac.ir/article-1-373-en.html
21. Nassereddine, M., Rizk, J., & Nagrial, M. *Conversion of a switched reluctance motor to operate as a generator for wind power applications*, 2009; 1–5. https://doi.org/10.1109/PTC.2009.5282005
22. Neto, P. J. D. S., Barros, T. A. D. S., De Paula, M. V., De Souza, R. R., & Filho, E. R. Design of Computational Experiment for Performance Optimization of a Switched Reluctance Generator in Wind Systems. *IEEE Transactions on Energy Conversion*, 2018; *33*(1): 406–419. https://doi.org/10.1109/TEC.2017.2755590
23. Omaç, Z., & Cevahir, C. Control of switched reluctance generator in wind power system application for variable speeds. *Ain Shams Engineering Journal*, 2021; *12*(3): 2665–2672. https://doi.org/10.1016/j.asej.2021.01.009
24. Padiyar, K. R. *Power System Dynamics Stability and Control* (secon edit). Bangalore, India: BS Publications, 2008; 4-4-309. Ginraj Lane, Sultan Bazar, Hyderabad.
25. Palanimuthu, K., Mayilsamy, G., Basheer, A. A., Lee, S. R., Song, D., & Joo, Y. H. A Review of Recent Aerodynamic Power Extraction Challenges in Coordinated Pitch, Yaw, and Torque Control of Large-Scale Wind Turbine Systems. *Energies*, 2022; *15*(21). https://doi.org/10.3390/en15218161
26. Pierre, A. D., Gilles, A. R., Théophile, H. K., & Antoine, V. Torque Ripple Minimization in Switch Reluctance Motor Using Model Predictive Control for Water Pumping Application. *Current Journal of Applied Science and Technology*, 2019; *32*(4): 1–9.

https://doi.org/10.9734/cjast/2019/44861

27. Pires, V. F., Pires, A. J., Cordeiro, A., & Foito, D. A Review of the Power Converter Interfaces for Switched Reluctance Machines. *Energies*, 2020; *13*(13). https://doi.org/10.3390/en13133490
28. Prabha Kundur. *Power System Stability And Control* (M. G. L. Neal J. Balu, ed.). Ontario, Toronto., 1994.
29. Reay, D S, Green, T. C., & Williams, B. W. Neural networks used for torque ripple minimisation from a switched reluctance motor. *1993 Fifth European Conference on Power Electronics and Applications*, 1993; 6: 1–6.
30. Reay, Donald S, Mirkazemi-moud, M., Green, T. C., & Williams, B. W. (1995). *Switched Reluctance Motor Control Via Fuzzy Adaptive Systems*. June, 2014. https://doi.org/10.1109/37.387611
31. Ro, H.-S., Lee, K.-G., Lee, J.-S., Jeong, H.-G., & Lee, K.-B. Torque Ripple Minimization Scheme Using Torque Sharing Function Based Fuzzy Logic Control for a Switched Reluctance Motor. *Journal of Electrical Engineering & Technology*, 2015; *10*(1): 118–127. https://doi.org/10.5370/JEET.2014.9.5.742
32. Saad, N. H., El-Sattar, A. A., & Metally, M. E. Artificial neural controller for torque ripple control and maximum power extraction for wind system driven by switched reluctance generator. *Ain Shams Engineering Journal*, 2018; *9*(4): 2255–2264. https://doi.org/10.1016/j.asej.2017.03.005
33. Sahoo, S., Dasgupta, S., Panda, S., & Xu, J.-X. A Lyapunov Function-Based Robust Direct Torque Controller for a Switched Reluctance Motor Drive System. *Power Electronics, IEEE Transactions On*, 2012; *27:* 555–564. https://doi.org/10.1109/TPEL.2011.2132740
34. Shahbazi, R. *A New Converter Based on DITC for improving Torque Ripple and Power Factor in Switched Reluctance Motors*, 2021.
35. Shin, H. U., Park, K., & Lee, K. B. A non-unity torque sharing function for torque ripple minimization of Switched Reluctance Generators in wind power systems. *Energies*, 2015; *8*(10): 11685–11701. https://doi.org/10.3390/en81011685
36. Susitra, D., Jebaseeli, E. A. E., & Paramasivam, S. Switched Reluctance Generator - Modeling, Design, Simulation, Analysis and Control a Comprehensive Review. *International Journal of Computer Applications*, 2010; *1*(3): 12–25. https://doi.org/10.5120/90-189
37. Tariq, I., Muzzammel, R., Alqasmi, U., & Raza, A. Artificial Neural Network-Based

Control of Switched Reluctance Motor for Torque Ripple Reduction. *Mathematical Problems in Engineering*, 2020; *2020*. https://doi.org/10.1155/2020/9812715

38. Tavakkoli, M. A., & Moallem, M. Torque ripple mitigation of double stator switched reluctance motor (DSSRM) using a novel rotor shape optimization. *2012 IEEE Energy Conversion Congress and Exposition (ECCE)*, 2012; 848–852. https://doi.org/10.1109/ECCE.2012.6342730
39. Torrey, D. A. Switched reluctance generators and their control. *IEEE Transactions on Industrial Electronics*, 2002; *49*(1): 3–14. https://doi.org/10.1109/41.982243
40. Xu, A., Shang, C., Chen, J., Zhu, J., & Han, L. A New Control Method Based on DTC and MPC to Reduce Torque Ripple in SRM. *IEEE Access*, 2019; *7:* 68584–68593. https://doi.org/10.1109/ACCESS.2019.2917317
41. Xue, X. D., Cheng, K. W. E., & Ho, S. L. Optimization and Evaluation of Torque-Sharing Functions for Torque Ripple Minimization in Switched Reluctance Motor Drives. *Power Electronics, IEEE Transactions On*, 2009; *24:* 2076–2090. https://doi.org/10.1109/TPEL.2009.2019581
42. Zainab M. Gwoma, Musa Mustapha, Umar A. Benisheikh, Babangida Modu, A. B. B. Modelling and assesment of Wind Energy Resource for Power distribution system. *World Journal of Engineering Rersearch and Technology (WJERT)*, 2017; *3*(6): 133–139.
43. Zhang, X., Yang, Q., Ma, M., Lin, Z., & Yang, S. A Switched Reluctance Motor Torque Ripple Reduction Strategy With Deadbeat Current Control and Active Thermal Management. *IEEE Transactions on Vehicular Technology*, 2019; 1. https://doi.org/10.1109/TVT.2019.2955218